Copper electromigration in polycrystalline copper sulfide

Leslie H. Allen and Ephraim Buhks

Citation: Journal of Applied Physics **56**, 327 (1984); doi: 10.1063/1.333967
View online: http://dx.doi.org/10.1063/1.333967
View Table of Contents: http://scitation.aip.org/content/aip/journal/jap/56/2?ver=pdfcov
Published by the AIP Publishing

Copper electromigration in polycrystalline copper sulfide

Leslie H. Allen
McDonnell Douglas Corporation, Microelectronic Center, St. Louis, Missouri 63166

Ephraim Buhks
Research and Development Center, B. F. Goodrich, Company, Brecksville, Ohio 44141

(Received 31 October 1983; accepted for publication 22 February 1984)

Measurements of the electrochemical potential distribution on polycrystalline $Cu_{2-\alpha}S$ have been made. It was found that the basic transport mechanism for ionic conduction at temperatures between 25–70 °C for single phase chalcocite can be modeled as a vacancy mechanism. The chemical diffusion coefficient of copper in coper sulfide depends on the stoichiometry of the material and exhibit Arrhenius-type activated temperature dependence with the activation energy $E_a = 0.45$ eV.

I. INTRODUCTION

The $CdS/Cu_{2-\alpha}S$ solar cell is a candidate for large scale solar energy conversion. A main concern at this point in the development of the cell for commercial use is the long term stability of the device. One major stability problem of the $Cu_{2-\alpha}S$/Cds cell is related to Cu^+ ion migration in the $Cu_{2-\alpha}S$ layer.[1]

$Cu_{2-\alpha}S$ is generally known as an ionic conductor at temperatures exceeding 100 °C. At room temperature the ionic conductivity[2] decreases by a factor 10^4 (from 10^{-1} Ω^{-1} cm^{-1} at 105 °C to 10^{-5} Ω^{-1} cm^{-1} at 15 °C)[2] yet Cu^+ migration can still affect cell performance when the device is used over extended periods of time. This paper is concerned with the transport properties of the $Cu_{2-\alpha}S$ layer and particularly the effects of lateral Cu^+ ion migration in the presence of an electric field.

The ionic conductivity in $Cu_{2-\alpha}S$ has been studied by many authors.[2–9] In this paper we will discuss two possible models of ionic transport in high stoichiometric ($\alpha < 7\times10^{-3}$) polycrystalline copper sulfide at room temperatures and compare the theoretical predictions with experimental results. This study includes measurements of the diffusion coefficient of the Cu^+ ion in $Cu_{2-\alpha}S$ and its dependence on stoichiometry and temperature.

II. EXPERIMENTAL PROCEDURE

The samples in this study were fabricated using the standard[10] "wet dip" process where $Cu_{2-\alpha}S$ is epitaxially grown onto a thin film of CdS. The resulting thin film of $Cu_{2-\alpha}S$ is nominally 2000 Å thick and is polycrystalline. The stoichiometry of the sample is increased by either plasma treatment[11] or heat treatments in an inert N_2 ambient. The stoichiometry is decreased by heat treatments in air at 125 °C.

Two grids were applied to the $Cu_{2-\alpha}S$ layer in an interdigitated configuration (Fig. 1.) allowing for a two terminal connection. The grids (electronic electrodes) consisted of 0.008-cm-diameter copper-based wire coated with a conductive polymer. The pair of grids were 5 cm long and spaced approximately 0.05 cm apart. The voltage profile between the two electrodes was measured using a point probe assembly capable of positioning the probe within 0.0025 cm. The probe consisted of a thin 0.003-cm-diameter copper wire tapered to a point and electroplated with gold.

Current is driven in the $Cu_{2-\alpha}S$ layer through the two grids. The leakage current which is shunted through the CdS-metal substrate path is less than 0.1%. To minimize the shunt conductance the device is operated in the dark and one of the grids is shorted to the substrate as shown in Fig. 1.

In the present scheme the current is kept constant while monitoring the time dependent voltage between the two grids. Similar results can be obtained by keeping the voltage constant.

III. STEADY STATE

A. Theory

$Cu_{2-\alpha}S$ is a p-type compositional semiconductor where the value α determines the concentration of free carri-

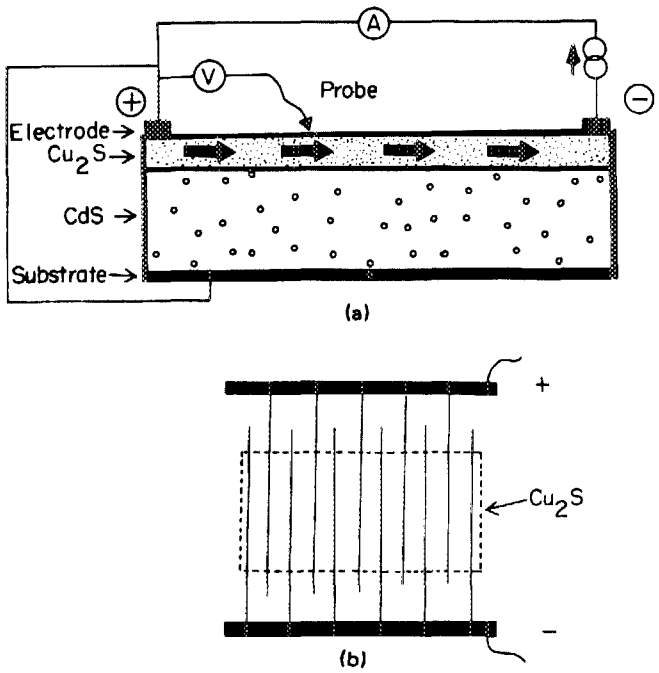

FIG. 1. (a) Setup for experimental study of lateral Cu^+ electromigration in $Cu_{2-\alpha}S$/CdS solar cell. (b) Interdigitated grid system for the study of Cu^+ electromigration in $Cu_{2-\alpha}S$.

 0021-8979/84/140327-09$02.40

ers C_1. The stoichiometry of the compound can be easily changed by adjusting the concentration of copper within the sample. When an electric potential is applied across a uniform sample, Cu^+ ions electromigrate toward the cathode. Subsequently the sample becomes nonuniform in composition, having higher Cu concentration near the cathode and lower concentration near the anode. This results in an inhomogeneous hole distribution between electrodes and an increase in voltage between electrodes.

The basic theory of mixed conductors has been developed by a number of authors.[12–14] The transport equation for $Cu_{2-\alpha}S$, a mixed conductor, can be written in the general form for electronic and ionic carriers as follows

$$J_n = -(\sigma_n/Z_n)\nabla\mu_n, \tag{1}$$

where J_n is current density, $\sigma_n = e\nu_n C_n|Z_n|$ is conductivity, ν_n is mobility, C_n is carrier concentration, $Z_n e$ is the charge of the carrier and $\nabla\mu_n$ is the gradient of electrochemical potential. The last factor $\nabla\mu_n$ can be divided into two parts, the gradient of the electrostatic potential $\Delta\varphi$ and the gradient in the chemical potential $\nabla\xi_n$

$$\nabla\mu_n = Z_n\nabla\varphi + \nabla\xi_n. \tag{2}$$

The index $n = 1,2$ stands for the electronic and ionic carriers, respectively. The gradient of the chemical potential can be represented as

$$\nabla\xi_n = A_n(kT/e)\nabla\ln(C_n), \tag{3}$$

where A_n is a thermodynamic factor $A_n = 1 + \partial\ln\gamma_n/\partial\ln C_n$ incorporating the activity coefficient γ_n. In the dilute limit $A_n = 1$ and the chemical diffusion coefficient is given by the Nernst–Einstein relation $D_n = kT\nu_n/e|Z_n|$. In the following derivations we consider a general case and show experimentally that the thermodynamic factors A_n for the electronic-ionic transport in $Cu_{2-\alpha}S$ are close to unity as expected in the dilute limit of $\alpha \ll 1$.

Equations (1) and (2) can be combined to give the general expression

$$J_1 = (\sigma_1/\sigma_T)J_T - (\sigma_1\sigma_2/\sigma_T)(\nabla\xi_1/Z_1 - \nabla\xi_2/Z_2), \tag{4}$$

where $\sigma_T = \sigma_1 + \sigma_2$ and $J_T = J_1 + J_2$.

Consider two models of ionic transport in $Cu_{2-\alpha}S$. In the electrolyte model, all of the Cu^+ ions ($Z_2 = 1$) in the crystal are involved in the transport process. The concentration of ionic carriers C_2 is of the order of 10^{22} cm^{-3} and therefore is almost independent of small changes in the composition. In this case the chemical potential of the Cu^+ ions is independent of composition and thus $\nabla C_2(x)$ is practically equal to zero. The transport equations can now be solved in terms of C_1. This model was applied to single crystals $Cu_{2-\alpha}S$ at high temperatures.[2]

The vacancy model assumes that only the negatively ionized copper vacancies ($Z_2 = -1$) are involved in the transport process. The transport equations can be solved assuming that the ionized vacancy concentration C_2 ($Z_2 = -1$) is equal to the hole concentration C_1 ($Z_1 = 1$), due to the local charge neutrality condition.

If constant current is maintained between two electrodes at a low value insufficient to electroplate copper at the cathode, then after a period of time the system comes to a steady state. The voltage between the electrodes increases and reaches a steady state value. The steady state condition implies that there is no ionic curent anywhere in the sample, $J_2(x/L) = 0$. The ionic carriers are blocked from leaving the system because the current-driving electrodes are electronic.

Under these conditions Eq. (1) can be reduced to the following equation:

$$J_1 = (kT/e)(\sigma_1/Z_1)(A_2Z_1\nabla C_2/Z_2C_2 - A_1\nabla C_1/C_1), \tag{5}$$

or

$$\nabla C_1 = -J_1/\nu_1 kTA_T, \tag{6}$$

where $A_T = A_1$ for the electrolyte model ($Z_1 = +1$, $Z_2 = +1$) and $A_T = A_1 + A_2$ for the vacancy model ($Z_1 = +1, Z_2 = -1$). If A_T and ν_1 (hole mobility) are independent of position, Eq. (1) and Eq. (6) can be combined to obtain an expression for A_T in terms of the measured quantities $\mu_1(x/L)$ and T:

$$1/A_T = -(kT/e)\nabla B(x/L), \tag{7}$$

where $B(x/L) = 1/\nabla\mu_1$. The accuracy in evaluation of A_T is limited by the accuracy of the measurement of $\mu_1(x/L)$. From this experimental technique the transport mechanism can be distinguished.

From Eq. (6) the steady-state hole concentration $C_1(x/L)$ is found to be a linear function of x

$$C_1(x/L)/\bar{C}_1 = 1 + (eV_0/A_TkT)(1/2 - x/L), \tag{8}$$

$$\bar{C}_1 = (1/L)\int_0^L C_1(x)dx, \tag{9}$$

where

$$V_0 = J_1L/\nu_1 e\bar{C}_1. \tag{10}$$

L is the distance between electrodes, $x/L = 0$ at the anode and $x/L = 1$ at the cathode. $\bar{C}_1$ is the average hole concentration in the steady state. The steady-state voltage profile $V_1(x/L)$ which is the electrochemical potential μ_1 relative to the anode, can be derived from Eq. (1)

$$V_1(x/L) = (A_TkT/e)\ln[C_1(0)/C_1(x/L)]. \tag{11}$$

From Eq. (11) the steady-state voltage $V_s = V_1(x/L = 1)$ between electrodes can be written in the following manner:

$$eV_0/2A_TkT = \tanh(eV_S/2A_TkT). \tag{12}$$

Usually $\bar{C}_1$ does not change during the course of the experiment. Then V_0 is simply the initial voltage between electrodes.

B. Experimental results

A sample with relatively high stoichiometry, characterized by $R_\square = 12\ k\Omega$, was polarized by constant current at 25 °C. The electrochemical potential profile $V_1(x/L)$ was measured between the cathode and anode before and after polarization. The current was held constant throughout the experiment. Initially the voltage is a linear function of x but in the polarized state the voltage increases rapidly near the cathode (Fig. 2).

From this data $B(x/L)$ was extracted (Fig. 3). The parameter A_T was evaluated to be $1.84 \pm 15\%$ by calculating the slope of $B(x)$. As a result within experimental error the vacancy model, where $A_T = 2$, appropriately describes the ionic transport mechanism in $Cu_{2-\alpha}S$ at 25 °C. At tempera-

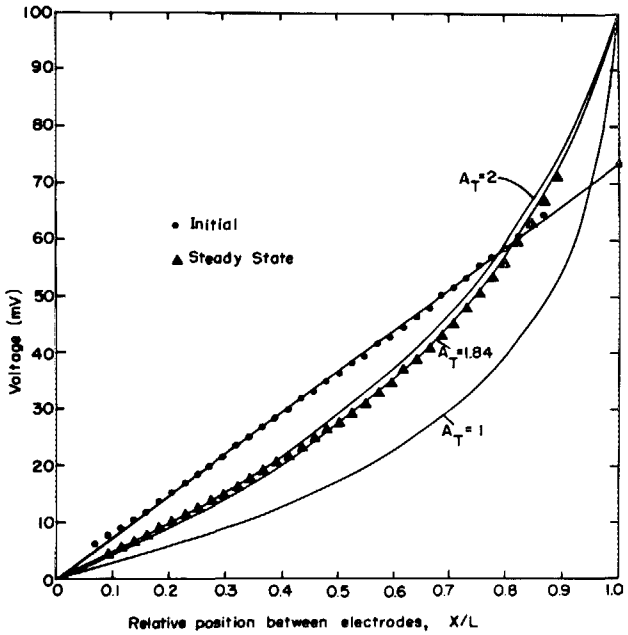

FIG. 2. Voltage (hole electrochemical potential) distribution in $Cu_{2-\alpha}S$ between the electrodes in constant current experiment for the initial (●) and steady-state (▲) conditions. Solid curves are calculated for various values of A_T [Eq. (11)].

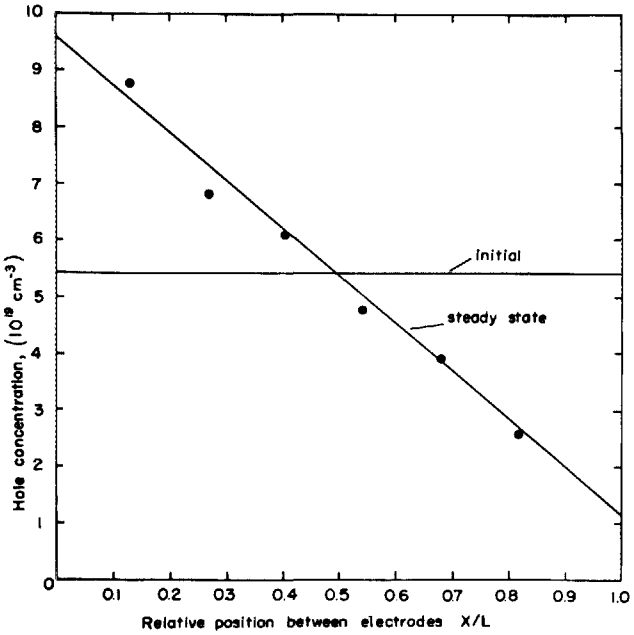

FIG. 4. Hole concentration in $Cu_{2-\alpha}S$ between electrodes at $t = 0$ and at the steady state.

tures above 100 °C, Yokota[13] found that the electrolyte model fits the experimental data.

The steady-state hole profile can now be determined using Eq. (8) and calculating $\bar{C}_1$ from Eq. (12). The predicted values, the solid line in Fig. 4, agree well with the experimental data determined from Eq. (1) and the $V_1(x/L)$ data. Shown in the same figure is the initial value of $\bar{C}_1$. Since $C_1(x/L)$ is linear then $C_1(x/L = 1/2) = \bar{C}_1$. It can be concluded from Fig. 4 that the average hole concentration, as expected, did not change during the experiment.

A comparison between observed and predicted values for the voltage distribution for $A_T = 1.84$ is shown in Fig. 2. $V_1(x/L)$ was calculated using Eqs. (11) and (8) for $A_T = 1,2$ keeping $\bar{C}_1$ constant, the same in all cases.

The initial and steady-state voltages were measured on several high stoichiometry samples where $R_\square > 10\,k\Omega$ (Fig. 5). The predicted relationship between V_0 and V_s is calculated from Eq. (12) for both models, assuming that $\bar{C}_1$ remains constant. There is good agreement of this experimental data with the vacancy model.

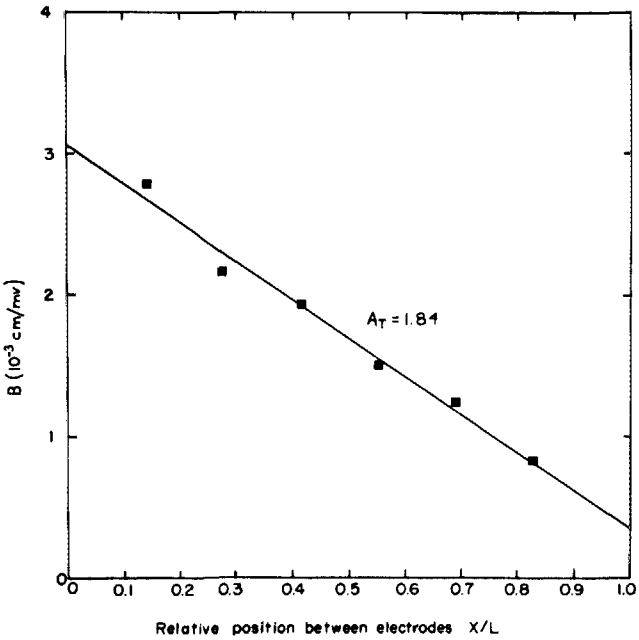

FIG. 3. Evaluation of A_T [Eq. (8)] from the steady-state voltage distribution.

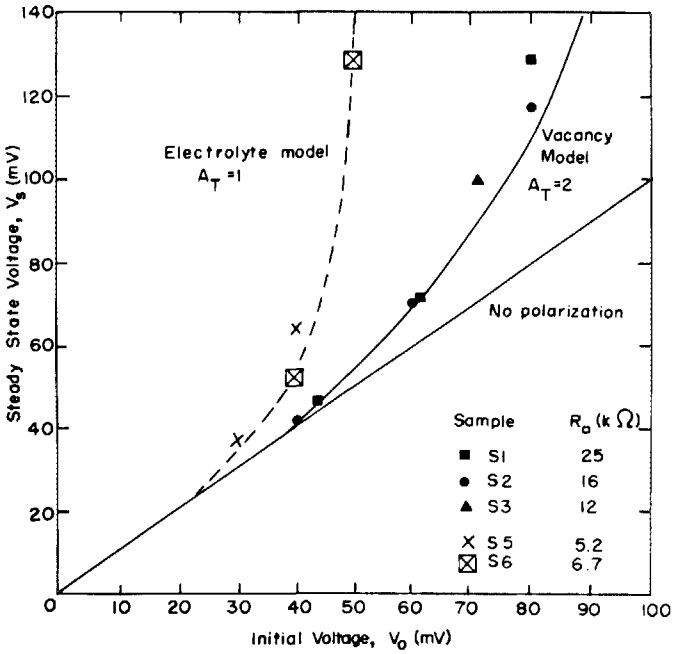

FIG. 5. Steady-state voltage in $Cu_{2-\alpha}S$ between electrodes vs the initial voltage in J = const experiment.

Also shown in Fig. 5 are the data for two low stoichiometry samples where $R_\square = 6.7$, 5.2 kΩ. The steady-state voltages of these samples are unexpectedly large compared to high stoichiometry samples. It appears as if the electrolyte model describes ionic electromigration in low stoichiometry samples. To determine whether the electrolyte is the correct model for these samples, A_T must be evaluated from the $V_1(x/L)$ data.

The voltage distribution $V_1(x/L)$ is measured on a low stoichiometry sample that has been polarized (Fig. 6). The parameter A_T is evaluated to be $1.76 \pm 15\%$ (Fig. 7) which is close to the vacancy model.

$C_1(x/L)$ is calculated using Eq. (8) and Eq. (12) by adjusting $\overline{C}_1$ and compared with the experimental data extracted using Eq. (1) (Fig. 8). Again there is good agreement between the data and the vacancy model. But the average hole concentration, which should equal $C_1(x/L = 1/2)$ is significantly lower (27%), than the initial value which is also shown in the figure.

The claim that $C_1(x/L = 1/2)$ decreases during polarization of low stoichiometry samples was verified by measurements using the sample as a photovoltaic device. The light-generated current I_L of the device is approximately inversely proportional to α. Therefore the hole concentration $C_1(X)$ can be indirectly measured in relative terms by measuring I_L. From the laser scanner[1] a relative profile $I_L(x/L)$ of a sample was measured before and after polarization (Fig. 9). The increase of $I_L(x/L = 1/2)$ midway between the electrodes confirms that the average hole concentration has decreased during polarization.

For the estimated values for A_T and $\overline{C}_1$ the calculated voltage profile in low stoichiometry samples is compared to the observed data (Fig. 6). The observed data agree with the predicted value within experimental error. Therefore it is concluded that in lower stoichiometry samples,

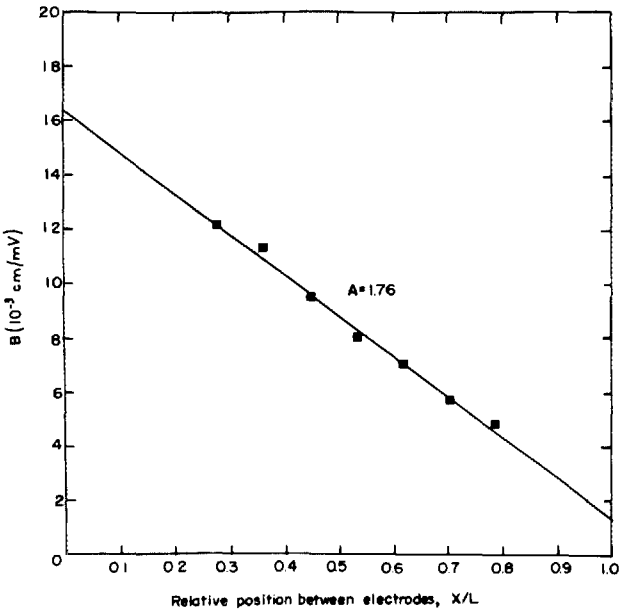

FIG. 7. Evaluation of A_T [Eq. (8)] from the steady-state voltage distribution measured on "low" stoichiometry $Cu_{2-\alpha}S$ sample.

$\alpha \gtrsim 7 \times 10^{-3}$, $\overline{C}_1$ decreases during polarization. It is also noted from Fig. 8 that the hole concentration increases almost to its initial value when the sample relaxes.

A number of measurements were performed on a pair of $Cu_{2-\alpha}S$ samples at various stoichiometry values, adjusted by heat treatments in air and by plasma treatment. The steady-state voltage resulting from the same initial voltage (40 mV) depends on the stoichiometry and is shown in Fig. 10. Note the sharp increase of V_s when the stoichiometry is near the mixed phase region ($R_\square < 6$ kΩ).

It is concluded from this data and the $V_1(x)$ data that the

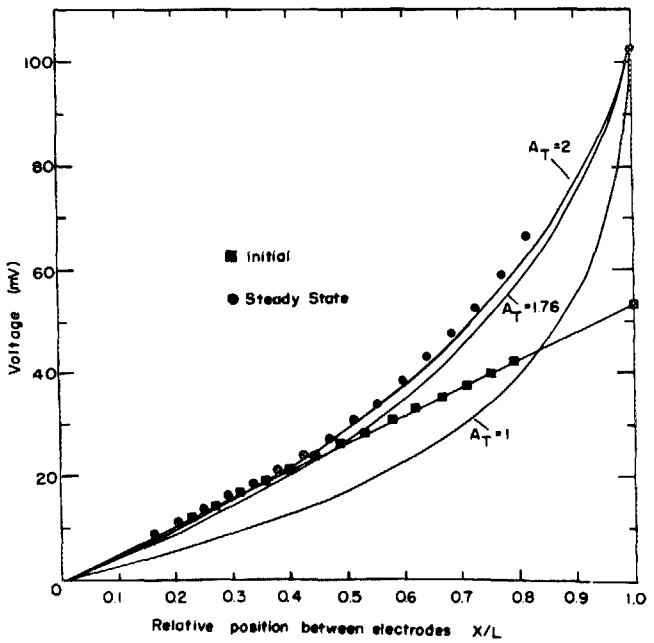

FIG. 6. Initial (▩) and steady-state (●) voltage distribution in "low" stoichiometry ($\alpha \simeq 0.01$) $Cu_{2-\alpha}S$. Solid curves are calculated using Eq. (11).

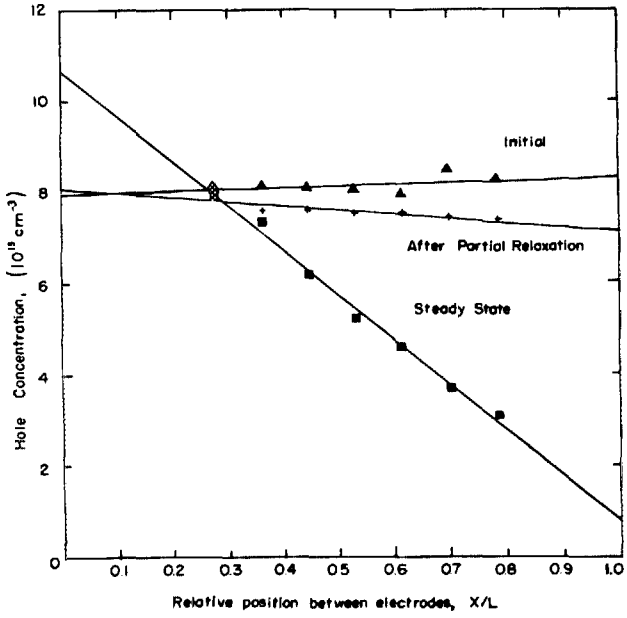

FIG. 8. Initial (▲), steady state (▩), and partially relaxed (+) hole concentration in low stoichiometry $Cu_{2-\alpha}S$.

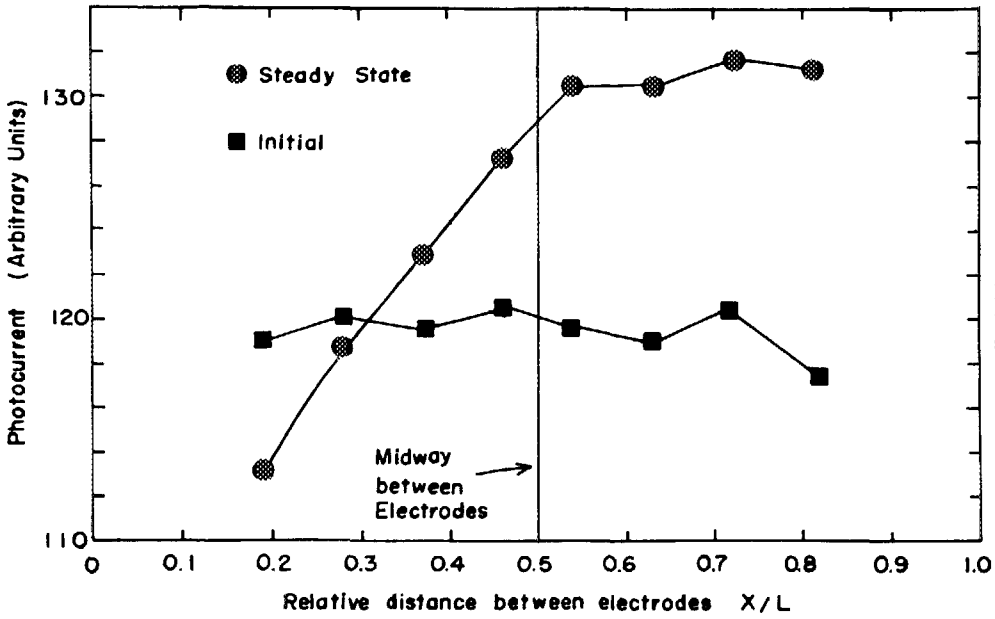

FIG. 9. Profile of light-generated current using a laser scanner of a polarized low stoichiometry sample.

factor A_T does not change with stoichiometry but that $\bar{C}_1$ changes during polarization if the low stoichiometry phase of copper sulfide Djurleite, is present.

Since these experiments were performed under controlled conditions it is unlikely that the average vacancy concentration $\bar{\alpha}$ changes during polarization. A decrease in $\bar{C}_1$ while $\bar{\alpha}$ remains constant during polarization can be explained by the nonlinear relationship between C_1 and α (in a uniform sample). The conductivity data σ_1 vs α of Rickert *et al.*[5] and Florio[6] in the chalcocite and Djurleite phases suggest that the ratio of ionized vacancies to the total number of vacancies decreases nonlinearly as α increases (assuming

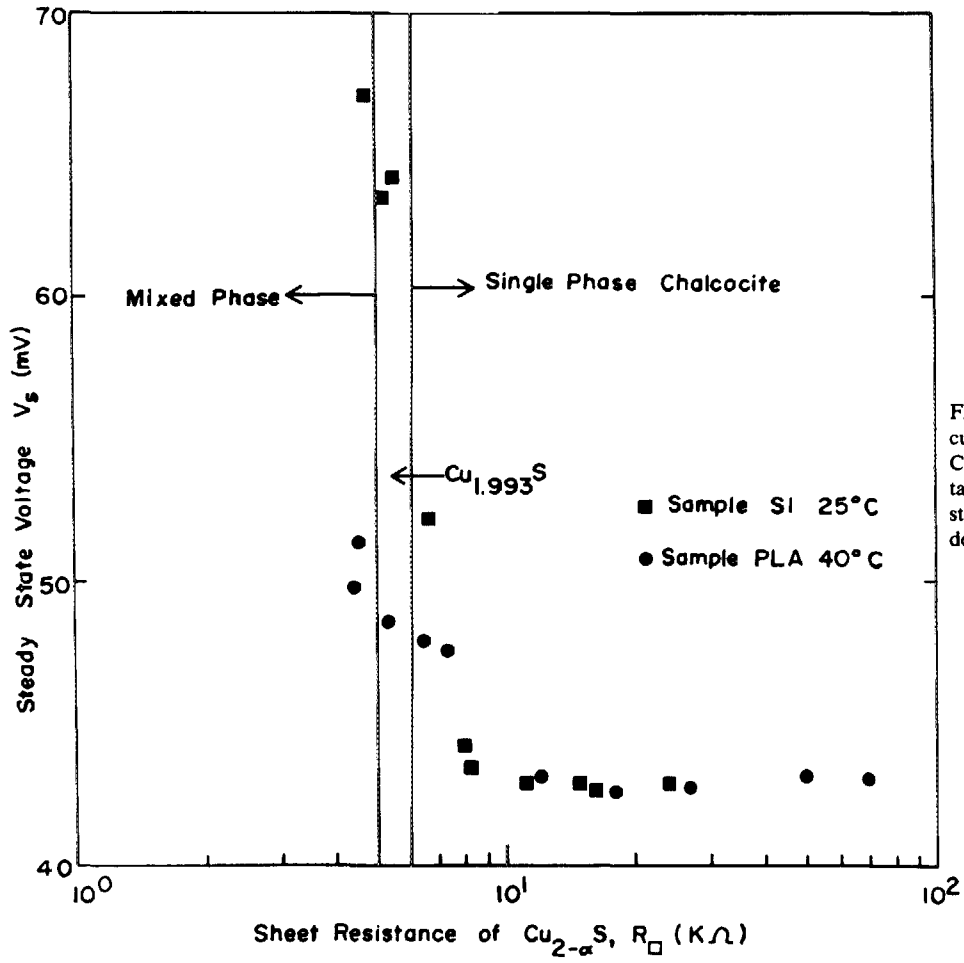

FIG. 10. The steady-state voltage data (constant current with $V_0 = 40.0$ mV) for samples of $Cu_{2-\alpha}S$ characterized by various sheet resistance, $R_\square$). The phase transition related to low stoichiometry $Cu_{2-\alpha}S$ at $R_\square \sim 5$–6 kΩ is evident.

that ν_1 remains constant). A consequence of this result is that during polarization the average number of ionized vacancies and holes will decrease yet the total number of vacancies remains constant. Charge neutrality is maintained since $C_1(x) = C_2(x)$. During polarization there will be a decrease in the average hole concentration but will return to its initial value during relaxation, as observed in our experiments.

IV. TIME DEPENDENCE

When constant current is maintained in a film of $Cu_{2-\alpha}S$ the voltage between the electrodes increases with time and then approaches a steady-state value. The hole concentration decreases near the cathode and increases near the anode. The time dependence of the net change in the concentration of holes and vacancies can be given by the continuity equation

$$\partial C_1/\partial t = -(1/e)\partial J_1/\partial x. \tag{13}$$

The standard diffusion equation can be obtained from Eqs. (4) and (13) by assuming that $\nabla J_T = 0$ so that charge neutrality is maintained

$$\partial C_1/\partial t = D\partial^2 C_1/\partial x^2, \tag{14}$$

where $D = 2D_2$ for the case of the vacancy model.

In order to find a unique solution to Eq. (14), for our boundary conditions it must be assumed that $\bar{C}_1$ remains constant during polarization. From the initial distribution $C(x/L) = \bar{C}_1$ and the final distribution of $C(x/L)$ given by Eq. (8) one can determine $C(x/L,t)$

$$C_1(x/L,t)/\bar{C}_1 = 1 + (eV_0/A_T kT) \times [1/2 - x/L - \phi(x/L,t/\tau)], \tag{15}$$

$$\phi(x/L,t/\tau) = (4/\pi^2)\sum\{\cos[(2m+1)\pi x/L]/(2m+1)^2\} \times \exp[-(2m+1)^2 t/\tau],$$

where $\tau = L^2/\pi^2 D$. An example of time and spacial dependence of hole concentration in $Cu_{2-\alpha}S$ with constant current density as calculated from Eq. (15), is displayed in Fig. 11 for $eV_0/A_T kT = 1.99$. The time dependence of voltage between the electrodes can be calculated from Eq. (1) by assuming that $J_T \simeq J_1$ since $\sigma_1 \gg \sigma_2$

$$V_1(t) = V_0 \int_0^1 d(x/L)[C_1(x/L,t)/\bar{C}_1]^{-1}. \tag{16}$$

The parameter τ was extracted from the experimental $V_1(x/L,t)$ data by curve fitting the data using numerical methods. Another way to determine τ is by an analytical expression for $V_1(x/L = 1,t)$ derived from Eqs. (16) and (11) by series expansion when $t/\tau > 1$

$$V_1(t) = V_S(1 - e^{-t/\tau}), \tag{17}$$

where V_S is the steady-state value of the voltage between electrodes. In Fig. 12 the predicted voltage-time characteristics are shown together with the observed data.

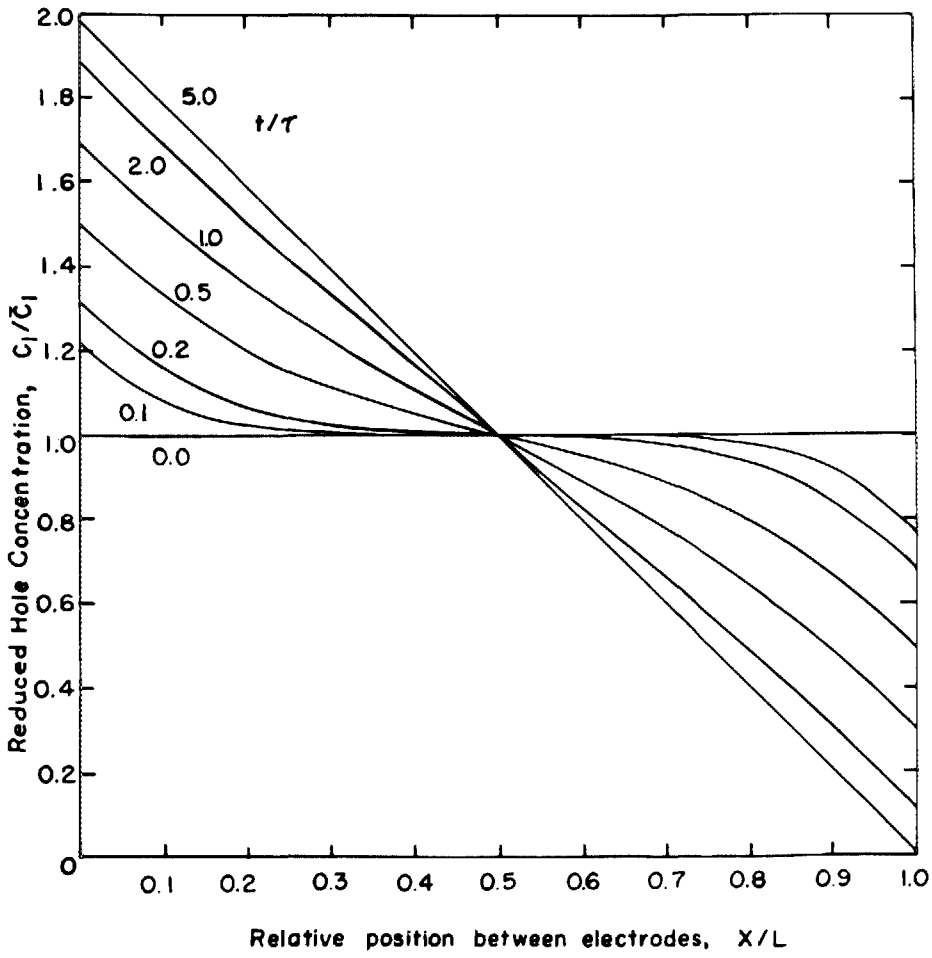

FIG. 11. Time and spatial dependence of hole concentration in CuS between electrodes under constant current, calculated from Eq. (15) for $eV_0/A_T kT = 1.99$.

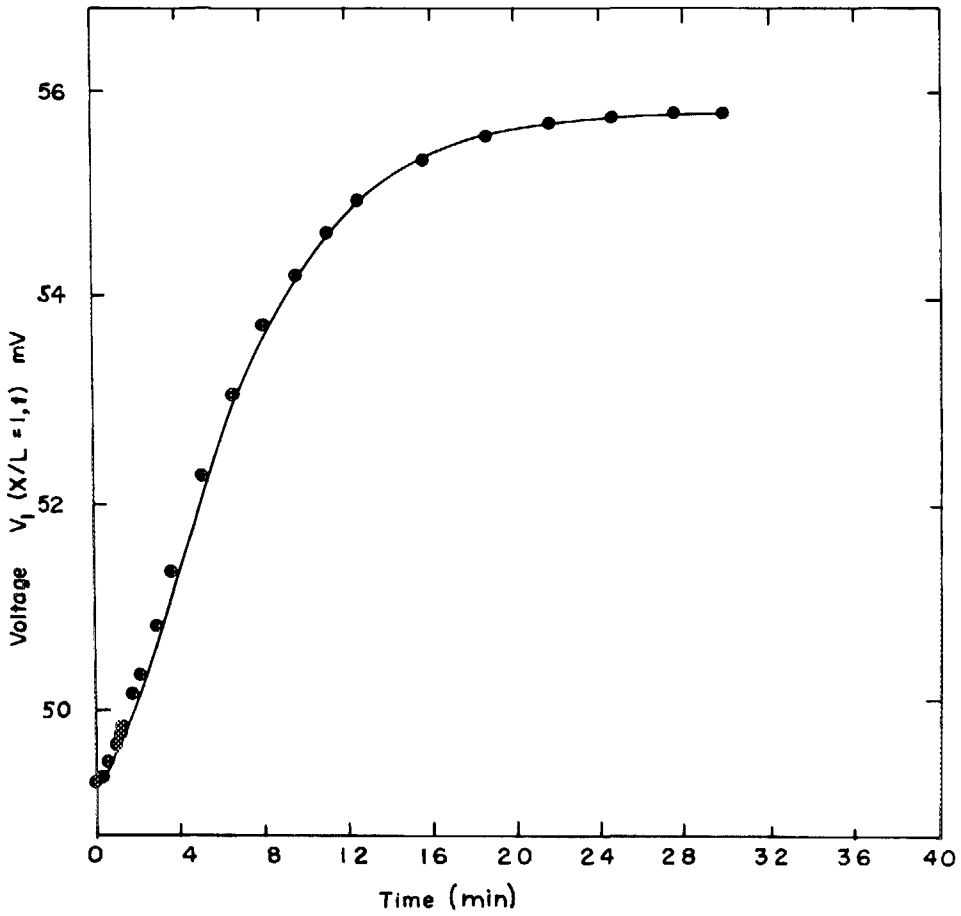

FIG. 12. Voltage kinetics during "polarization" of $Cu_{2-\alpha}S$ in $J = \text{const}$ experiment at $T = 298.5$ K. Experimental data (●) is fitted by theoretical curve calculated from Eqs. (15) and (16) with the parameters $A_T = 1.71$, $\tau = 4.4$ min.

The steady state is reached for practical purposes when $t/\tau > 5$. Then if the current is suddenly discontinued or reduced to some small value, the system relaxes and the hole concentration again becomes uniform. The rate of relaxation can be monitored by measuring the voltage between electrodes while maintaining a small current. $C_1(x,t)$ for the relaxation process can be determined by using the continuity Eq. (13) with the boundary conditions given by Eq. (8)

$$C_1(x,t)/\overline{C}_1 = 1 + (eV^0/A_T kT)(1/2 - x/L) + (e/A_T kT)(V_0 - V^0)\phi(x/L, t/\tau), \quad (18)$$

where $V^0 = V_0 J^1/J_1$ and J^1 is the relaxation current. Inserting Eq. (18) into Eq. (16) gives the voltage relaxation curve. As evident in Fig. 13, this result, calculated using τ from the polarization data agrees well with the observed data.

When the current is discontinued for a polarized $Cu_{2-\alpha}S$ sample at temperatures exceeding 100 °C [15] as expected from Eq. (1) and (4), there exists a residual voltage

$$V_r = (A_T kT/e)[\sigma_2/(\sigma_2 + \sigma_1)]\ln[C_1(0)/C_1(1)]. \quad (19)$$

This voltage in our experiments was too small to measure since $\sigma_2/\sigma_1 < 10^{-5}$ at room temperatures.

The diffusion coefficient was evaluated from τ at various temperatures and stoichiometries. it was shown earlier that for high stoichiometry material $\overline{C}_1$ was conserved during polarization. This is a necessary condition in order to obtain a unique solution for Eq. (14). Apparently $\overline{C}_1$ is not conserved in low stoichiometry samples and therefore the value for D_2 extracted from the voltage-time data may deviate from the actual value of chemical diffusion coefficient.

We assume the standard relationship between D_2 and T.

$$D_2 = D_0 \exp(-E_a/kT). \quad (20)$$

The results of the temperature experiments on two samples over a range of stoichiometries are shown in Fig. 14. The activation energy was calculated for each experiment and was found to vary between 0.4 and 0.5 eV when the samples were in the single phase region. This compares to 0.45 and 0.24 eV as reported by Rickert *et al.*[5] and Okamoto and Kawai.[4] $D_0 = 30$ cm^2/sec for $E_a = 0.45$ eV.

When the sample is either oxidized or reduced in the single phase region D_2 changes almost linearly with $R_\square$ as seen in Fig. 15. A similar result has been observed by others.[4–6] Although it was clear that D_2 changed in a systematic way with stoichiometry, it could not be established whether D_0 and/or E_a was responsible for the changes, due to the large experimental error.

There is an anomalous decrease in D_2 as the stoichiometry approaches the mixed phase boundary $Cu_{1.993}S$. Since $\overline{C}_1$ does not remain constant during polarization, for this case there is no unique solution $C_1(x,t)$. The values for D_2 extracted from the $V_1(t)$ data for the low stoichiometry samples may be some average of the diffusion coefficient of each phase. D_2 has been determined using other techniques[7]: for single phase chalcocite $Cu_{1.993}$ $D_2 = 6\times10^{-9}$ and for single phase djurleite $Cu_{1.965}$ $D_2 = 2.4\times10^{-10}$ cm^2/s (Ref. 6). Our values for D_2 in polycrystalline $Cu_{2-\alpha}S$ at room temperature vary two orders of magnitude from 2×10^{-9} cm^2/sec ($R_\square = 4.5$ kΩ) to 2×10^{-7} cm^2/sec ($R_\square = 70$ kΩ). These

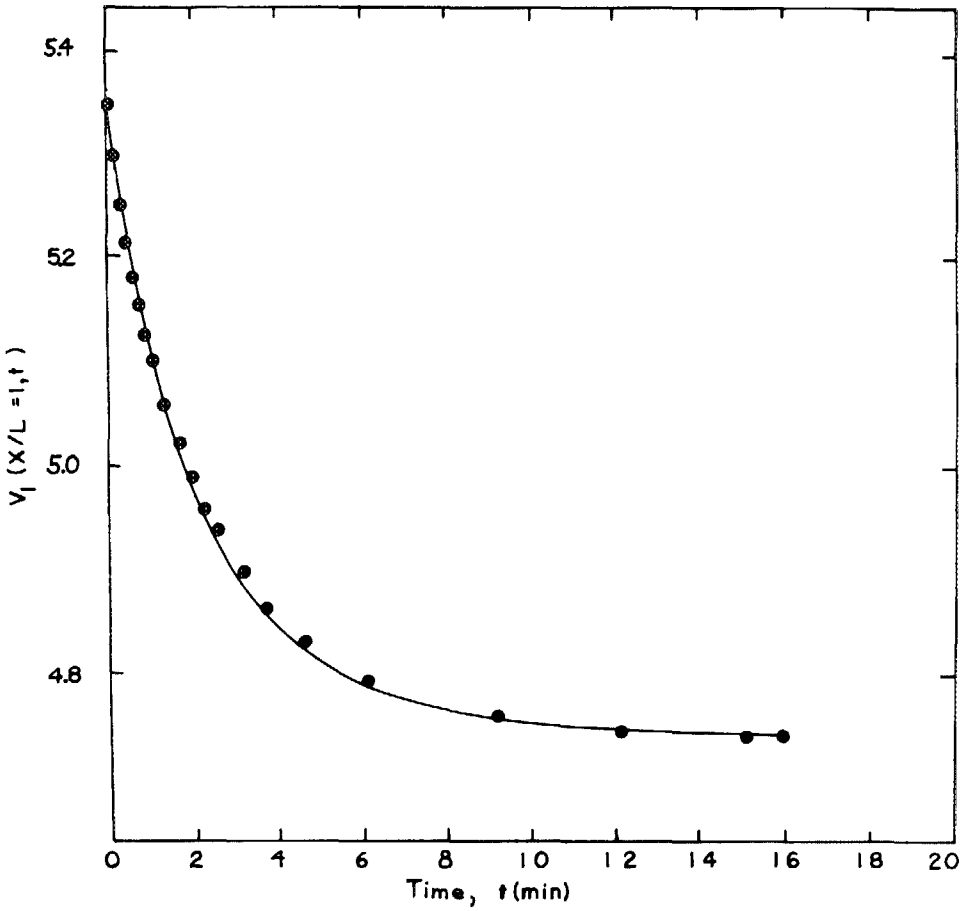

FIG. 13. Voltage kinetics during relaxation of $Cu_{2-\alpha}S$ when the current was decreased tenfold after the steady state was established (Fig. 12). Theoretical curve [Eqs. (18) and (16)] was calculated using the same value of τ as in Fig. 12.

results are also in agreement with Rickert *et al.*[5] data $D_2 = 1.5\times10^{-6}$ cm^2/sec for $Cu_{2.000}S$ and $D_2 = 2\times10^{-8}$ cm^2/sec for $Cu_{1.93}S$.

There are several approaches that may be used in relating stoichiometry with D_2 in single-phase chalcocite. One approach used to understand this problem relates the factors

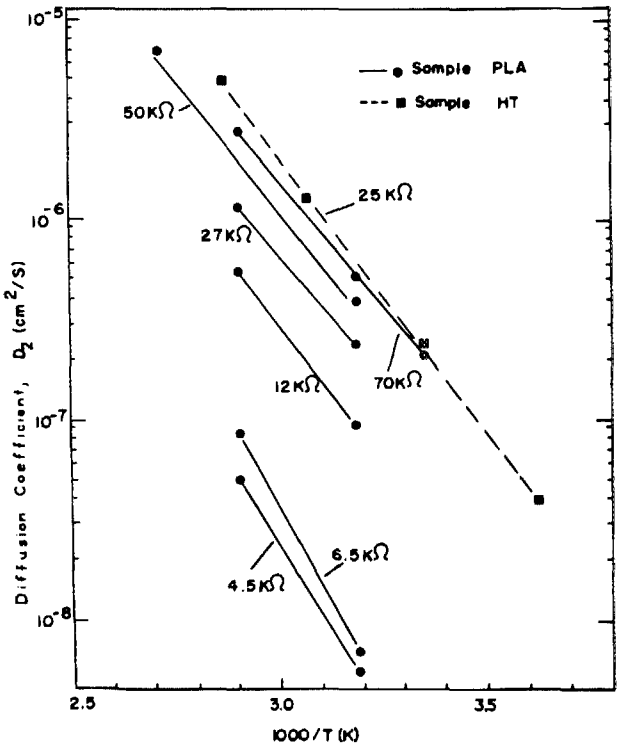

FIG. 14. Temperature dependence of copper diffusion coefficient in 2 samples of $Cu_{2-\alpha}S$ at various stoichiometries characterized by sheet resistance.

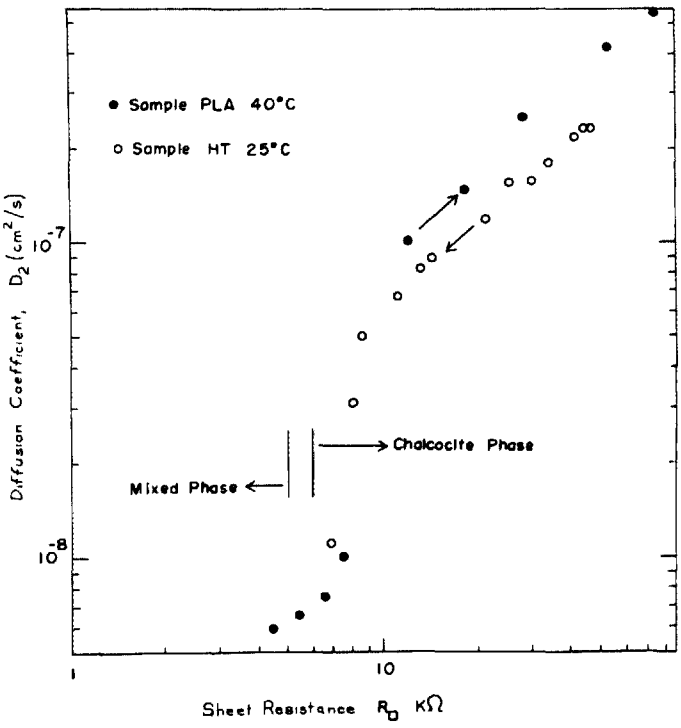

FIG. 15. Copper diffusion coefficient vs sheet resistance of 2 samples at various stoichiometries.

D_0 and E_a [Eq. (19)] directly to the value α. $D_0 = r^2\omega$, where r is the elementary jump distance and ω is the vibrational frequency. If r is given to be the average distance between vacancies, then $D_0 \propto \alpha^{-2/3}$. Therefore when α decreases, D_2 should increase. In addition to this, charge transfer theory[16,17] in ionic media predicts that

$$E_a = (e^2/16\pi\epsilon_0)(1/n^2 - 1/\epsilon)(1/a - 1/r_0), \tag{21}$$

where n is the index of refraction, ϵ is the dielectric constant, a is the radius of the exchanging ion, and r_0 is the distance between ions. Therefore, if r_0 is equal to the average distance between vacancies, then as α decreases, D_2 should increase.

However it should be noted that there are other approaches used to investigate ionic transport in relation to changes in stoichiometry. J. Florio[6] has been able to relate the chemical diffusion coefficient with the tracer diffusion coefficient by measuring ionic conductivity of $Cu_{2-\alpha}S$ via an electrochemical cell.[18]

V. CONCLUSION

One can determine the ionic transport mechanism in the $Cu_{2-\alpha}S$ mixed conductor by measuring the electrochemical potential distribution of the holes in a polarized sample. The method which has been described here has the advantage that the results are independent of the presence of contact resistances at the electrodes and changes of current density and/or stoichiometry, which may occur during experiments.

With this method it is concluded that the vacancy model adequately describes the effects of polarization for $Cu_{2-\alpha}S$ samples between 25–70 °C. Also it it shown that when the sample is in the mixed phase region there is a decrease in the average hole concentration during polarization.

Finally, it was found that the diffusion coefficient of samples in the single phase Chalcocite region varies linearly with sheet resistance. The temperature dependence exhibits the Arrhenius law relationship with activation energy of 0.4–0.5 V.

ACKNOWLEDGMENTS

This work was done at SES Inc., Newark, Delaware. The authors would like to acknowledge K. Boer, J. Bragagnolo, J. Van Oosterhout, D. Garcia, L. DeFillipo, U. Pernisz, J. Womac, and especially J. Florio for many useful technical discussions and support. The technical assistance of B. Hirshout and F. Willing is greatly appreciated.

[1]H. Zwicker, L. A. Brickman, H. C. Hadley, and K. J. Matysik, Proceedings of the 15th IEEE PV Spec. Conference, Orlando, Fla., **787**, (1981).
[2]S. Miyatani, J. Phys. Soc. Jpn. **11**, 1059 (1956).
[3]E. Hirahara, J. Phys. Soc. Jpn. **6**, 422 (1951).
[4]K. Okamota and S. Kawai, Jpn. J. Appl. Phys. **12**, 1130 (1973).
[5]H. Rickert, I. Schmidt, R. Wagner, and H. Weimhofer, Proceedings of the International PV Conference, Stresa, Italy, 1982.
[6]J. Florio (unpublished).
[7]E. Castel, International Conference PV Sol. Engineering, Luxembourg, 1977.
[8]A. Etienne, J. Electrochem. Soc., **117**, 870 (1970).
[9]L. Hmurcik, L. Allen, and R. Serway, J. Appl. Phys. **53**, 9063 (1982).
[10]W. E. Devaney, A. Barnett, G. M. Storti, and J. Meakin, IEEE Trans. Electron Devices **26**, 205 (1979).
[11]K. Bogus and S. Mattes, Proceedings 9th PV Spec. Conference, Silver Springs, Md., 1972.
[12]M. H. Hebb, J. Chem. Phys. **29**, 185 (1952).
[13]I. Yokota, J. Phys. Soc. Jpn. **16**, 2213 (1961).
[14]G. J. Dudley and B. C. H. Steele, J. Solid State Chem. **31**, 331 (1980).
[15]I. Yokota, J. Phys. Soc. Jpn. **8**, 595 (1953).
[16]R. A. Marcus, Annual. Rev. Phys. Chem. **15**, 155 (1964).
[17]E. Buhks, M. Bixon, J. Jortner, and G. Navon, Inorg. Chem. **18**, 2014 (1979).
[18]W. F. Chu, H. Rickert, and W. Weppner, in *Fast Ion Transport in Solids*, edited by W. vanGool (North Holland, New York, 1973), p. 181.